Journal of Environmental Management 92 (2011) 1237–1247

Contents lists available at ScienceDirect

Journal of Environmental Management

journal homepage: www.elsevier.com/locate/jenvman

# Application of cupuassu shell as biosorbent for the removal of textile dyes from aqueous solution

Natali F. Cardoso [a], Eder C. Lima [a,*], Isis S. Pinto [a], Camila V. Amavisca [a], Betina Royer [a], Rodrigo B. Pinto [a], Wagner S. Alencar [b], Simone F.P. Pereira [b]

[a] Institute of Chemistry, Federal University of Rio Grande do Sul, UFRGS, Av. Bento Gonçalves 9500, Caixa Postal 15003, CEP 91501-970, Porto Alegre, RS, Brazil
[b] Institute of Exact and Natural Sciences, Federal University of Para, UFPA, Belem, PA, Brazil

ARTICLE INFO

*Article history:*
Received 11 July 2010
Received in revised form
15 November 2010
Accepted 12 December 2010
Available online 31 December 2010

*Keywords:*
Biosorption
Cupuassu shell
Textile dyes
Nonlinear isotherm fitting
Adsorption kinetics

ABSTRACT

The cupuassu shell (Theobroma grandiflorum) which is a food residue was used in its natural form as biosorbent for the removal of C.I. Reactive Red 194 and C.I. Direct Blue 53 dyes from aqueous solutions. This biosorbent was characterized by infrared spectroscopy, scanning electron microscopy, and nitrogen adsorption/desorption curves. The effects of pH, biosorbent dosage and shaking time on biosorption capacities were studied. In acidic pH region (pH 2.0) the biosorption of the dyes were favorable. The contact time required to obtain the equilibrium was 8 and 18 h at 298 K, for Reactive Red 194 and Direct Blue 53, respectively. The Avrami fractionary-order kinetic model provided the best fit to experimental data compared with pseudo-first-order, pseudo-second-order and chemisorption kinetic adsorption models. The equilibrium data were fitted to Langmuir, Freundlich, Sips and Radke–Prausnitz isotherm models. For both dyes the equilibrium data were best fitted to the Sips isotherm model.



## 1. Introduction

Dyes are one of the most hazardous chemical compound class found in industrial effluents which need to be treated since their presence in water bodies reduces light penetration, precluding the photosynthesis of aqueous flora (Pavan et al., 2008; Royer et al., 2009a, 2009b, 2010a). They are also aesthetically objectionable for drinking and other purposes. Dyes can also cause allergy, dermatitis, skin irritation and also provoke cancer and mutation in humans (Brookstein, 2009; de Lima et al., 2007; Rosenkranz et al., 2007).

Dyes are a kind of organic compound with a complex aromatic molecular structure that can bring bright and firm color to other materials. However, the complex aromatic molecular structures of dyes make them more stable and more difficult to biodegrade (Calvete et al., 2010; Royer et al., 2010b). The most efficient method for the removal of synthetic dyes from aqueous effluents is the adsorption procedure (Al-Degs et al., 2008; Cestari et al., 2009; Mittal et al., 2010; Rosa et al., 2008). This process transfers the dyes from the water effluent to a solid phase thereby keeping the effluent volume to a minimum (Al-Degs et al., 2008; Calvete et al., 2010). Subsequently, the adsorbent can be regenerated or stored in a dry place without direct contact with the environment (Calvete et al., 2009, 2010).

Activated carbon is the most employed adsorbent for dye removal from aqueous solution because of its excellent adsorption properties (Calvete et al., 2009, 2010; Órfão et al., 2006; Olivares-Marín et al., 2009). However, the extensive use of activated carbon for dye removal from industrial effluents is expensive, limiting its large application for wastewater treatment (Crini, 2006; Gupta and Suhas, 2009). Therefore, there is a growing interest in finding alternative low cost adsorbents for dye removal from aqueous solution. Among these alternative adsorbents, it can be cited: hazelnut shell, saw dust, walnut, saw dust cherry, saw dust oak, saw dust pitch pine, saw dust pine, cane pitch, soy meal hull, banana pitch (Gupta and Suhas, 2009); sugar cane bagasse, cotton waste, chitin and chitosan, peat, microorganisms such as fungus and yeasts (Crini, 2006); maize cob (Crini, 2006; Gupta and Suhas, 2009); Brazilian pine-fruit shell (Lima et al., 2008; Royer et al., 2009b, 2010c); mandarin peel, yellow passion fruit peel (Pavan et al., 2007); tree leaves (Deniz and Saygideger, 2010); wood shavings (Janoš et al., 2009); coffee bean (Baek et al., 2010); babassu (Vieira et al., 2009); marine algae (Bekçi et al., 2009) etc.

Cupuassu (*Theobroma grandiflorum*), is a tropical rainforest tree related to cacao (Gondim et al., 2001), native in the Brazilian Amazon. Cupuassu trees usually range from 5 to 15 m in height (Gondim et al., 2001), and cupuassu fruits are oblong, brown, and

* Corresponding author. Tel.: +55 (51) 3308 7175; fax: +55 (51) 3308 7304.
*E-mail addresses:* eder.lima@ufrgs.br, profederlima@gmail.com (E.C. Lima).

0301-4797 
doi:10.1016/j.jenvman.2010.12.010

fuzzy. They are 20 cm long, 1–2 kg in weight, and covered with a thick (4–7 mm) hard exocarp (Gondim et al., 2001). The pulp is greatly appreciated for its pleasant acidic taste, being consumed fresh or processed, mainly as juice, ice cream, candy and jellies. In addition, the seeds can be used to make chocolate. The annual production of cupuassu in the Brazilian Amazon is about 5200 tonnes (Gondim et al., 2001). About 42% of weight of cupuassu is its shell, which is a waste material that presents no aggregate economic value (Gondim et al., 2001). The disposal of large amounts of cupuassu shell (CS) directly in the soil and/or in natural waters may contaminate the environment in an uncontrolled way because the decomposition of this waste material leads to the generation of various chemical compounds and microorganisms. In this context, combining the need to reduce costs with commercial adsorbents and by using CS as biosorbent for the removal of dyes from industrial effluents, it is a good economical and environmental advantage to in developing countries such as Brazil.

The present work aimed to use CS in natural form as biosorbent for the successful removal of C.I. Direct Blue 53 (DB-53) and C.I. Reactive Red 194 (RR-194) dyes from aqueous solutions. These dyes are largely used for textile dying in the Brazilian cloth industries.

## 2. Materials and methods

### 2.1. Solutions and reagents

De-ionized water was used throughout the experiments for solution preparations.

The textile dyes, C.I. Reactive Red 194 (RR-194; C.I. 18214; CAS 23354-52-1; $C_{27}H_{18}N_7O_{16}S_5ClNa_4$; 984.21 g mol$^{-1}$) was furnished by Bosche Scientific (New Brunswick, USA) at 80% of purity and C.I. Direct Blue 53 (DB-53; C.I. 23860; CAS 314-13-6; $C_{34}H_{24}N_6O_{14}S_4Na_4$; 960.81 g mol$^{-1}$) was furnished by Vetec (Rio de Janeiro, Brazil) at 85% of purity (see Supplementary Fig. 1). The dyes were used without further purification. It should be pointed out that no color changes of the dyes were observed when these were immersed in aqueous solution ranging from pH 2.0 to 9.0. The RR-194 dye has three sulfonate groups and one sulfato-ethyl-sulfone group, and the DB-53 has four sulfonate groups. These groups present negative charges even in highly acidic solutions due to their pKa values lower than zero (Lima et al., 2008). The stock solution was prepared by dissolving the dyes in distilled water to the concentration of 5.00 g L$^{-1}$. Working solutions were obtained by diluting the dye stock solutions to the required concentrations. To adjust the pH solutions, 0.10 mol L$^{-1}$ sodium hydroxide or hydrochloric acid solutions were used. The pH of the solutions was measured using a Schott Lab 850 set pHmeter.

### 2.2. Adsorbent preparation and characterization

CS was furnished by jelly industry in Belém-PA, Brazil, as a residual material. CS was washed with tap water to remove dust and with de-ionized water. Then, it was dried at 343 K in an air-supplied oven for 8 h. After that, CS was grounded in a disk-mill and subsequently sieved. The part of biosorbent which presented diameter of particles $\leq$ 250 μm was used.

The CS biosorbent was characterized by FTIR using a Shimadzu FTIR, model 8300 (Kyoto, Japan). The spectra were obtained with a resolution of 4 cm$^{-1}$, with 100 cumulative scans.

The surface analyses and porosity were carried out with a volumetric adsorption analyzer, ASAP 2020, from Micromeritrics, at 77 K (boiling point of nitrogen). The samples were pre-treated at 373 K for 24 h under a nitrogen atmosphere in order to eliminate the moisture adsorbed on the solid sample surface. After, the samples were submitted to 298 K in vacuum, reaching the residual pressure of $10^{-4}$ Pa. For area and pore calculations, the DBET and BJH (Arenas et al., 2007; Jacques et al., 2007) methods were used.

The biosorbent sample was also analyzed by scanning electron microscopy (SEM) in Jeol microscope, model JSM 6060, using an acceleration voltage of 20 kV and magnification ranging from 100 to 5000 fold (Vaghetti et al., 2008).

The point of zero charge ($pH_{pzc}$) of the adsorbent was determined by adding 20.00 mL of 0.050 mol L$^{-1}$ NaCl to several Erlenmeyer flasks. A range of initial pH ($pH_i$) values of the NaCl solutions were adjusted from 2.0 to 10.0 by adding 0.1 mol L$^{-1}$ of HCl and NaOH. The total volume of the solution in each flask was brought to exactly 30.0 mL by further addition of 0.050 mol L$^{-1}$ NaCl solution. The $pH_i$ values of the solutions were then accurately noted and 50.0 mg of CS was added to each flask, which was securely capped immediately. The suspensions were shaken in a shaker at 298 K and allowed to equilibrate for 48 h. The suspensions were then centrifuged at 3600 rpm for 10 min and the final pH ($pH_f$) values of the supernatant liquid were recorded. The value of $pH_{pzc}$ is the point where the curve of $\Delta pH$ ($pH_f - pH_i$) versus $pH_i$ crosses the line equal to zero (Calvete et al., 2009).

### 2.3. Biosorption studies

The biosorption studies for evaluation of the CS biosorbent for the removal of the RR-194 and DB-53 dyes from aqueous solutions were carried out in triplicate using the batch contact biosorption method. For these experiments, fixed amounts of biosorbent (20.0–200.0 mg) were placed in 50.0 mL cylindrical high-density polystyrene flasks (height 117 mm and diameter 30 mm) containing 20.0 mL of dye solutions (10.00–250.0 mg L$^{-1}$), which were agitated for a suitable time (0.25–48 h) at 298 K. Blanks without adsorbents were carried out in order to verify the possibility of the dye being adsorbed at the flask. It was not observed any adsorption of the dye at the high-density polystyrene flask after 48 h of contact. The pH of the dye solutions ranged from 2.0 to 9.0. Subsequently, in order to separate the biosorbents from the aqueous solutions, the flasks were centrifuged at 3600 rpm for 10 min, and aliquots of 1–10 mL of supernatant were properly diluted with water.

The final concentrations of the dyes remained in the solution were determined by visible spectrophotometry by visible spectrophotometry using a T90+ UV–VIS spectrophotometer furnished by PG Instruments (London-England) provided with optical quartz cells. Absorbance measurements were made at the maximum wavelength of RR-194 and DB-53 which were 505 and 607 nm.

The amount of dyes uptaken and the percentage of removal of the dyes by the biosorbent were calculated by applying the Eqs. (1) and (2), respectively:

$$q = \frac{\left(C_o - C_f\right)}{X} \quad (1)$$

$$\%\text{Removal} = 100 \cdot \frac{\left(C_o - C_f\right)}{C_o} \quad (2)$$

where $q$ is the amount of dyes taken up by the biosorbent (mg g$^{-1}$); $C_o$ is the initial dye concentration put in contact with the adsorbent (mg L$^{-1}$), $C_f$ is the dye concentration (mg L$^{-1}$) after the batch adsorption procedure, and X is biosorbent dosage (g L$^{-1}$).

### 2.4. Kinetic and equilibrium models

Avrami fractionary-order (Lopes et al., 2003), pseudo-first-order (Largegren, 1898), pseudo-second-order (Blanachard et al., 1984), Elovich-chemisorption (Vaghetti et al., 2009) and intra-particle

**Table 1**
Kinetic adsorption models.

| Kinetic model | Nonlinear equation |
|---|---|
| Fractionary-order | $q_t = q_e \cdot \{1 - \exp[-(k_{AV} \cdot t)]^{n_{AV}}\}$ |
| Pseudo-first order | $q_t = q_e \cdot [1 - \exp(-k_f \cdot t)]$ |
| Pseudo-second-order | $q_t = \frac{k_s \cdot q_e^2 \cdot t}{1 + q_e \cdot k_s \cdot t}$ <br> $h_o = k_s \cdot q_e^2$ <br> initial sorption rate |
| Chemisorption | $q_t = \frac{1}{\beta}(\alpha \cdot \beta) + \frac{1}{\beta}(t)$ |
| Intra-particle diffusion | $q_t = k_{id} \cdot \sqrt{t} + C$ |

diffusion model (Weber and Morris, 1963.) kinetic equations are given in Table 1.

Langmuir (Langmuir, 1918), Freundlich (Freundlich, 1906), Sips (Sips, 1948) and Radke–Prausnitz (Radke and Prausnitz, 1972.) isotherm equations are given in Table 2.

### 2.5. Quality assurance and statistical evaluation of the kinetic and isotherm parameters

To establish the accuracy, reliability and reproducibility of the collected data, all the batch adsorption measurements were performed in triplicate. Blanks were run in parallel and they were corrected when necessary (Vaghetti et al., 2008).

All dye solutions were stored in glass flasks, which were cleaned by soaking in 1.4 mol $L^{-1}$ $HNO_3$ for 24 h (Lima et al., 2002), rinsing five times with de-ionized water, dried, and stored in a flow hood.

For analytical calibration, standard solutions with concentrations ranging from 5.00 to 50.0 mg $L^{-1}$ of RR-194 and DB-53 dyes were employed, running against a blank solution of water adjusted in a suitable pH. The linear analytical calibrations of the curves were furnished by the software UVWin of the T90 + PG Instruments spectrophotometer. The detection limits of the method, obtained with signal/noise ratio of 3 (Lima et al., 1998), were 0.12 and 0.16 mg $L^{-1}$, for RR-194 and DB-53, respectively. All the analytical measurements were performed in triplicate, and the precision of the standards was better than 3% ($n = 3$). For checking the accuracy of the RR-194 and DB-53 dye sample solutions during the spectrophotometric measurements, standards containing dyes at 20.00 mg $L^{-1}$ were employed as quality control at each five determinations (Lima et al., 2003).

The kinetic and equilibrium models were fitted by employing a nonlinear method, with successive interactions calculated by the method of Levenberg–Marquardt and also interactions calculated by the Simplex method, using the nonlinear fitting facilities of the software Microcal Origin 7.0. In addition, the models were also evaluated by adjusted determination factor ($R^2_{adj}$), as well as by an error function ($F_{error}$) (Lima et al., 2007), which measures the differences in the amount of dye taken up by the adsorbent predicted by the models and the actual $q$ measured experimentally. $R^2_{adj}$ and $F_{error}$ are given below, respectively:

**Table 2**
Isotherm models.

| Isotherm model | Equation |
|---|---|
| Langmuir | $q_e = \frac{Q_{max} \cdot K_L \cdot C_e}{1 + K_L \cdot C_e}$ |
| Freundlich | $q_e = K_F \cdot C_e^{1/n_F}$ |
| Sips | $q_e = \frac{Q_{max} \cdot (K_S \cdot C_e)^{1/n_S}}{1 + (K_S \cdot C_e)^{1/n_S}}$ |
| Radke–Prausnitz | $q_e = \frac{Q_{max} \cdot K_{RP} \cdot C_e}{(1 + K_{RP} \cdot C_e)^{1/n_{RP}}}$ |

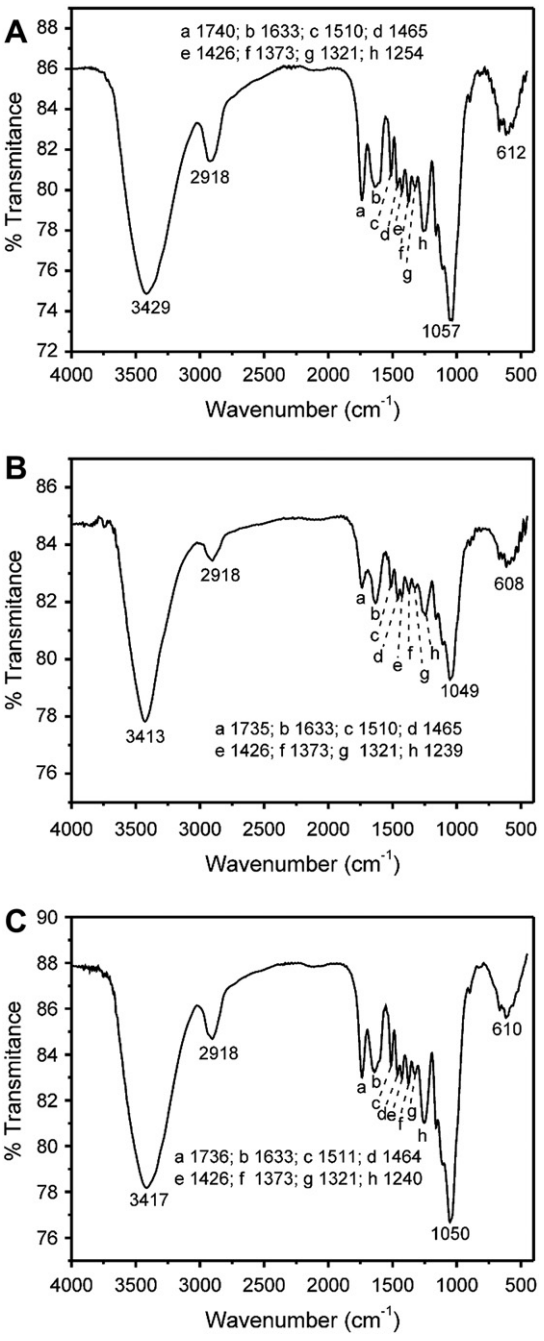


**Fig. 1.** FTIR vibrational spectra. A) CS before the adsorption; B) CS + RR-194 after the adsorption; C) CS + DB-53 after the adsorption. The number indicated for the bands correspond to wavenumbers that are expressed in $cm^{-1}$.

$$R^2_{adj} = 1 - \left( \frac{\sum_i^n \left(q_{i,exp} - q_{model}\right)^2}{\sum_i^n \left(q_{i,exp} - \overline{q}_{exp}\right)^2} \right) \cdot \left( \frac{n-1}{n-p} \right) \quad (3)$$

$$F_{error} = \sqrt{\left( \frac{1}{n-p} \right) \cdot \sum_i^n \left(q_{i,exp} - q_{imodel}\right)^2} \quad (4)$$

where $q_{i,model}$ is the value of $q$ predicted by the fitted model, $q_{i,exp.}$ is the value of $q$ measured experimentally, $\overline{q}_{exp}$ is the average of $q$

experimentally measured, $n$ is the number of experiments performed, and $p$ is the number of parameter of the fitted model.

## 3. Results and discussion

### 3.1. Characterization of biosorbents

FTIR technique was used to examine the surface groups of CS biosorbent and to identify the groups responsible for the dyes adsorption. Infrared spectra of the adsorbent and dye-loaded adsorbent samples, before and after the adsorption process, were recorded in the range 4000–400 $cm^{-1}$. Fig. 1A–C shows the FTIR vibrational spectra of the CS before the adsorption (CS; Fig. 1A) and loaded with the RR-194 dye (CS + RR-194; Fig. 1B) and with DB-53 (CS + DB-53, Fig. 1C). The intense absorption bands at 3429, 3413, and 3417 $cm^{-1}$ are assigned to O–H bond stretching for CS, CS + RR-194 and CS + DB-53, respectively (Smith, 1999; Vaghetti et al., 2009; Lima et al., 2008). The $CH_2$ stretching band at 2918 $cm^{-1}$ is assigned to asymmetric stretching of $CH_2$ groups (Smith, 1999; Vaghetti et al., 2008; Lima et al., 2008) which present the same wavenumber before and after the adsorption with two different dyes, indicating that this group did not participate in the biosorption process. Bands at 1740, 1735 and 1736 $cm^{-1}$, for CS, CS + RR-194 and CS + DB-53, respectively are assigned to carbonyl groups of carboxylic acid (Smith, 1999; Vaghetti et al., 2009). Several bands in the range of 1633-1321 are assigned to ring modes of the aromatic rings (Smith, 1999). The wavenumbers of these bands were practically the same before and after the biosorption using RR-194 and DB-53 dyes, indicating that aromatic groups do not participate on the biosorption mechanism. A sharp band at 1254, 1239 and 1240 $cm^{-1}$ as well as the intense bands at 1057, 1049 and 1050 $cm^{-1}$ are assigned to C–O stretch of phenolic compounds found in lignin (Smith, 1999; Vaghetti et al., 2009) and C–O stretching vibration of alcohols (Smith, 1999), for CS, CS + RR-194 and CS + DB-53, respectively. The FTIR results indicate that the interaction of RR-194 and DB-53 dyes with the CS biosorbent should occur with the O–H bonds of phenols and alcohols present in the lignin structure as well as the interactions with the carboxylate group because these groups suffered a shift to lower wavenumbers after the biosorption procedure. Similar results were previously observed for adsorption of dyes on fly ash (Kara et al., 2007) and activated carbon adsorbent (Calvete et al., 2010).

The textural properties of CS obtained by nitrogen adsorption/desorption curves were: superficial area ($S_{BET}$) 1.2 $m^2\ g^{-1}$; average pore diameter (BJH) 20.02 nm; and average pore volume 0.0073 $cm^3\ g^{-1}$. The superficial area of agricultural residues is usually a low value (Kumari et al., 2006; Yurtsever and Sengil, 2009). On the other hand, the average pore diameter of CS biomaterial is relatively large, even when compared with activated carbons (Calvete et al., 2009; 2010) or silicates (Royer et al., 2010a, 2010b). The maximum diagonal lengths of the RR-194 and DB-53 (see supplementary Fig. 2. The dimensions of the chemical moleculae were calculated using ChemBio 3D® Ultra version 11.0.) are 2.05 and 1.47 nm, respectively. The ratios of average pore diameter of the biosorbent to the maximum diagonal length of each dye are 9.77 and 13.62, for RR-194 and DB-53, respectively. Therefore, the mesopores of CS could accommodate up to 9 and 13 molecules of RR-194 and DB-53, respectively. This number of molecules, which could be accommodated in each pore of the biosorbent, is considered large when compared with other adsorbents reported in the literature (Calvete et al., 2009, 2010; Lima et al., 2008; Royer et al., 2009b).

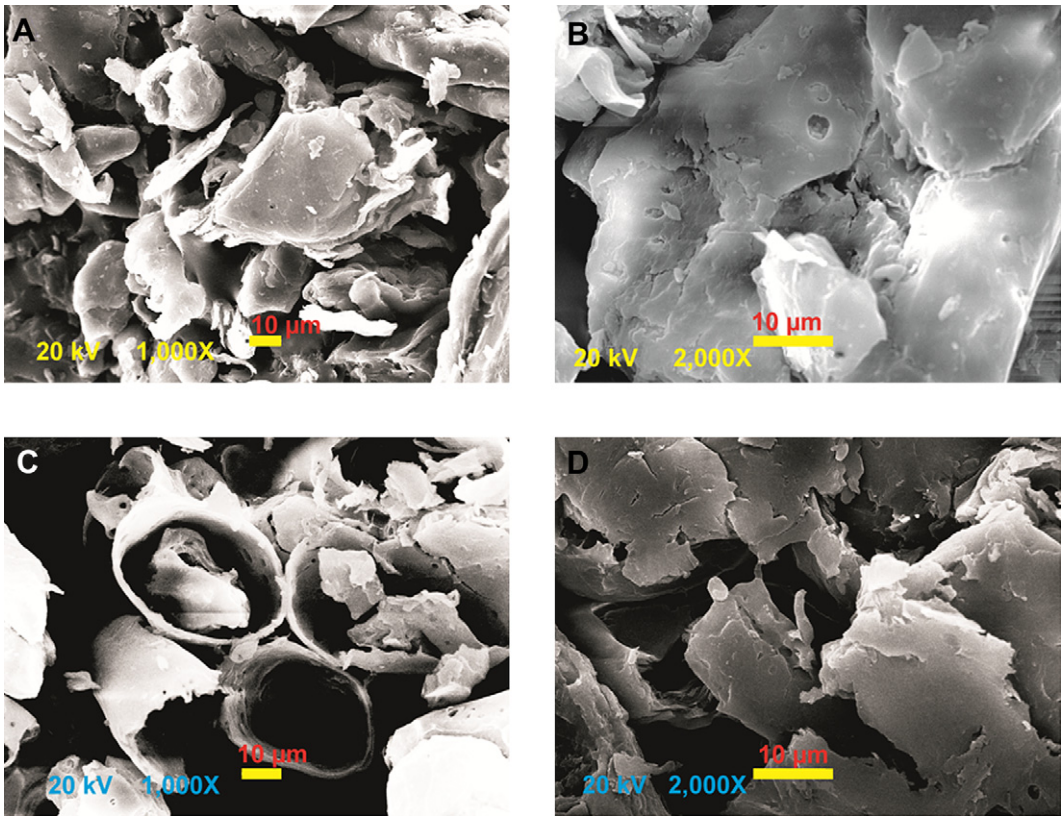


**Fig. 2.** SEM of CS. A) without contact with dye solution, magnification 1,000×; B) without contact with dye solution, magnification 2,000×; C) after contact with RR-194 dye solution (pH 2.0) for 12 h, magnification 1000×; D) after contact with RR-194 dye solution (pH 2.0) for 12 h, magnification 2000×.

Scanning electron microscopies (SEM) of the biosorbent in natural form without contact with dye solution (Fig. 2A and B) and after contact with RR-194 dye solution at pH 2.0 (Fig. 2C and D) are shown in Fig. 2. As can be seen, CS biosorbent without contact with dye solution is a more compact fibrous material presenting some macroporous (porous with diameter $>$ 50 nm; see Fig. 2A and B). On the other hand, after the CS biosorbent being submitted to an RR-194 dye solution at pH 2.0, the cavities of the fibrous materials were expanded, which should allow the diffusion of dye molecules through the macroporous of the CS biosorbent. Similar results were also obtained with DB-53 after the contact with CS biosorbent (data not shown). It is important to focus that using SEM technique it is not possible to verify the presence of dye on the biosorbent surface, since the scale of the micrograph is micrometers and the dimension of the dyes are in nanometer scale. The changes provoked at cupuassu shell (cavities) should be attributed to the acidic solution at pH 2.0.

Taking into account that CS biosorbent presents a low superficial area ($S_{BET}$) and some macroporous (see Fig. 2), it could be inferred that CS predominates a mixture of mesoporous (porous with diameter ranging from 2 to 50 nm, see textural results described above) and macroporous (porous with diameter $>$ 50 nm). On the other hand, the number of microporous (porous with a diameter $<$ 2 nm) should be a minimum (Gay et al., 2010; Jacques et al., 2007). Usually, the microporous structure is responsible for higher superficial area ($S_{BET}$) of the materials (Gay et al., 2010; Kumari et al., 2006; Yurtsever and Sengil, 2009), since the nitrogen probe molecule utilized in the measurements is retained basically at the microporous structure (Arenas et al., 2007; Jacques et al., 2007). This explains the low superficial area ($S_{BET}$) of CS biosorbent.

### 3.2. Effects of acidity on adsorption

One of the most important factors in adsorption studies is the effect of the acidity of the medium (Lima et al., 2007, 2008; Royer et al., 2009a, 2009b). Different species may present divergent ranges of suitable pH depending on which adsorbent is used. Effects of initial pH on percentage of removal of RR-194 and DB-53 dyes using CS biosorbent were evaluated within the pH range between 2 and 9 (Fig. 3A and B, respectively). For both dyes, the percentage of dye removal was remarkably decreased from pH 2.0, attaining practically less than 1% of dye removal at pH 6.5. Similar behavior for dye removal utilizing lignocellulosic adsorbents was also observed (Akar et al., 2008; Deniz and Saygideger, 2010).

The $pH_{PZC}$ value determined for CS is 5.92. For pH values lower than $pH_{pzc}$, the adsorbent presents a positive surface charge (Calvete et al., 2009; Lima et al., 2008). The dissolved RR-194 and DB-53 dyes are negatively charged in water solutions. The adsorption of these dyes takes place when the biosorbent presents a positive surface charge. For CS, the electrostatic interaction occurs for pH $<$ 5.92. However, the lower the pH value from the $pH_{pzc}$, the more positive the surface of the biosorbent (Calvete et al., 2009).

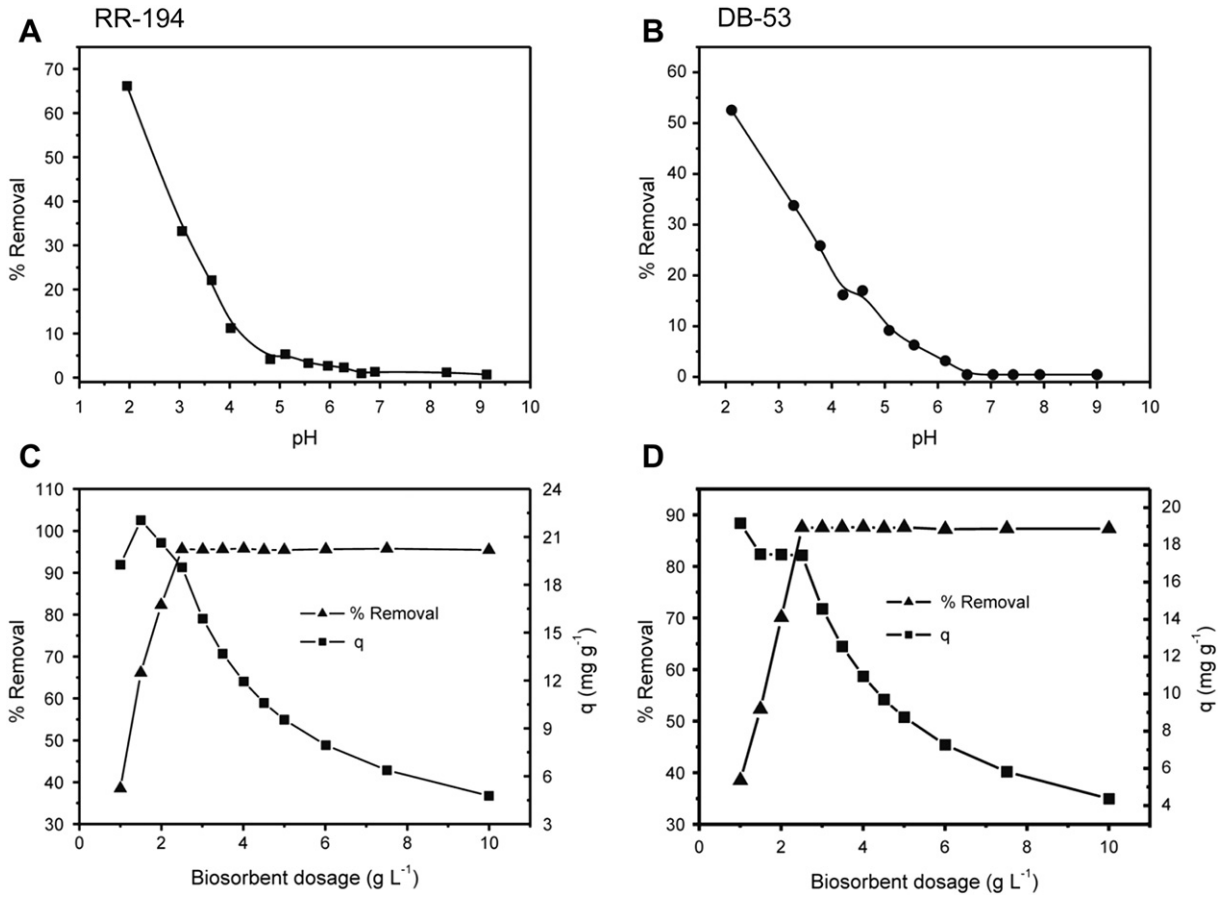


**Fig. 3.** Optimization of biosorption conditions. Effect of pH on the biosorption of RR-194 (A) and DB-53 (B). Effect of the biosorbent dosage on the percentage of removal and in the amount adsorbed of RR-194 (C) and DB-53 (D). Conditions: A) and B) $C_o$ = 50.0 mg $L^{-1}$ and mass of biosorbent of 30.0 mg for both dyes. C) and D) $C_o$ = 50.0 mg $L^{-1}$, pH 2.0 for both dyes. The temperature was fixed at 298 K.

This behavior explains the high sorption capacity of CS for both RR-194 and DB-53 at pH 2. In order to continue the biosorption studies, the initial pH was fixed at 2.0.

### 3.3. Adsorbent dosage

The study of biosorbent dosages for the removal of RR-194 and DB-53 dyes from aqueous solution was carried out using biosorbent dosages ranging from 1.0 to 10.0 g $L^{-1}$ and fixing the initial dye concentration at 50.0 mg $L^{-1}$. For both dyes, the highest amount of dye removal was attained for biosorbent doses of at least 2.5 g $L^{-1}$ (Fig. 3C and D, for RR-194 and DB-53, respectively). For biosorbent dosages higher than this value, the removal of the dyes remained almost constant. Increases in the percentage of the dye removal with biosorbent dosages could be attributed to increases in the biosorbent surface areas, augmenting the number of adsorption sites available for adsorption, as already reported in several papers (Lima et al., 2008; Royer et al., 2009b, 2010b; Vaghetti et al., 2008, 2009). On the other hand, the increase in the biosorbent doses promotes a remarkable decrease in the amount of dye uptake per gram of adsorbent ($q$), (Fig. 3C and D), an effect that can be mathematically explained by combining the Eqs. (1) and (2):

$$q = \frac{\%\text{Removal} \cdot C_o}{100 \cdot X} \quad (5)$$

As observed in the Eq. (5), the amount of dye uptaken ($q$) and the biosorbent dosage (X) is inversely proportional. For a fixed dye percentage removal (after doses of 2.5 g $L^{-1}$), the increase of biosorbent doses leads to a decrease in $q$ values, since the initial dye concentration ($C_o$) is always fixed. These results clearly indicate that the biosorbent dosages must be fixed at 2.5 g $L^{-1}$, which is the biosorbent dosage that corresponds to the minimum amount of adsorbent that leads to constant dye removal. Biosorbent dosages were therefore fixed at 2.5 g $L^{-1}$ for both dyes.

### 3.4. Kinetic studies

Adsorption kinetic studies are important in the treatment of aqueous effluents because they provide valuable information on the mechanism of the adsorption process (Calvete et al., 2009, 2010; Vaghetti et al., 2009).

In attempting to describe the biosorption kinetics of RR-194 and DB-53 dyes by CS biosorbent, four diffusion kinetic models were tested, as shown in Fig. 4A and B (RR-194); 4C, 4F (DB-53). The kinetic parameters for the kinetic models are listed in Table 3. Based on the $F_{error}$ values, it was observed that the Avrami model provides the best fit to the data for using RR-194 and DB-53 dye, because its $F_{error}$ values were at least 3.18 and 3.11 times lower, for RR-194 and DB-53, respectively than the values obtained for pseudo-first-order, pseudo-second-order and Elovich-chemisorption kinetic models. The lower the error function, the lower the difference of the $q$ calculated by the model from the experimentally measured $q$ (Lima et al., 2007, 2008; Calvete et al., 2009, 2010). It should be pointed out that the $F_{error}$ utilized in this work takes into account the number of the fitted parameter (p term of Eq. (4)), since it is reported in the literature (Gunay, 2007) that depending on the number of parameters one nonlinear equation presents, it has the best fitting of the results (Gunay, 2007). For this reason, the number of fitted parameter should be considered in the calculation of $F_{error}$. Also, it was verified that the $q_e$ values found in the fractionary-order were closer to the experimental $q_e$ values, when compared with all other kinetic models. These results indicate that the fractionary-order kinetic model should explain the adsorption process of RR-194 and DB-53 using CS biosorbent.

The Avrami kinetic equation has been successfully employed to explain several kinetic processes of different adsorbents and adsorbates (Calvete et al., 2009, 2010; Cestari et al., 2005; Lopes et al., 2003; Lima et al., 2008; Royer et al., 2009a, 2009b, 2010a, 2010b; Vaghetti et al., 2009). The Avrami exponent ($n_{AV}$) is a fractionary number related with the possible changes of the adsorption mechanism that takes place during the adsorption process (Calvete et al., 2009, 2010; Lima et al., 2008). Instead of following only an integer-kinetic order, the mechanism adsorption could follow multiple kinetic orders that are changed during the contact of the adsorbate with the adsorbent (Calvete et al., 2009, 2010; Lima et al., 2008). The $n_{AV}$ exponent is a resultant of the multiple kinetic order of the adsorption procedure.

Since kinetic results fit very well to the fractionary kinetic model (Avrami model) for the RR-194 and DB-53 dyes using CS as biosorbent (Table 3 and Fig. 4), the intra-particle diffusion model (Vaghetti et al., 2009) was used to verify the influence of mass transfer resistance on the binding of RR-194 and DB-53 dyes to the biosorbent (Table 3 and Fig. 4C,D,G and H). The intra-particle diffusion constant, $k_{id}$ (mg $g^{-1}$ $h^{-0.5}$), can be obtained from the slope of the plot of $q_t$ (uptaken at any time, mg $g^{-1}$) versus the square root of time. Fig. 4C and D (RR-194); 4G, 4H (DB-53) shows the plots of $q_t$ versus $t^{1/2}$, with multi-linearity for the RR-194 and DB-53 dyes using CS biosorbent. These results imply that the adsorption processes involve more than one single kinetic stage (or adsorption rate) (Vaghetti et al., 2009). For the DB-53 dye, the adsorption process exhibits three stages, which can be attributed to each linear portion of the Fig. 4G and H. The first linear portion was attributed to the diffusional process of the dye to the CS biosorbent surface (Vaghetti et al., 2009); hence, it was the fastest sorption stage. The second portion, ascribed to intra-particle diffusion, was a delayed process. The third stage may be regarded as the diffusion through smaller pores, which is followed by the establishment of equilibrium. For RR-194 dye, the adsorption process exhibits only two stages, being the first linear part attributed to intra-particle diffusion, and the second stage the diffusion through smaller pores, which is followed by the establishment of equilibrium (Vaghetti et al., 2009).

It was observed in Fig. 4 that the minimum contact time of RR-194 and DB-53 with the CS biosorbent to reach equilibrium was about 8 and 18 h, respectively. This great difference in the minimum contact time to reach the equilibrium is associated with the difference in the mechanism of adsorption. The Avrami constant rate ($k_{AV}$) for RR-194 was 29.4% higher than the $k_{AV}$ for DB-53 dye, which implies that the diffusion from the film could not explain completely the remarkable differences on the kinetics of adsorption of RR-194 in relation to DB-53. On the other hand, the intra-particle diffusion constant ($k_{id}$) for RR-194 was more than 9-fold higher than the $k_{id}$ for DB-53, indicating that the resistance to the mass transfer is much lower for RR-194 dye. This could explain the difference of 10 h to reach the equilibrium for RR-194 in relation to DB-53. Probably DB-53 molecules should be more aggregated, forming dimers in aqueous solution, which would increase the resistance to the mass transfer inside the porous of CS biosorbent (Murakami, 2002).

In order to continue this work, the contact time between the biosorbent and biosorbates was fixed at 10.0 and 20.0 h using RR-194 and DB-53 dyes as biosorbates, respectively and CS as biosorbent to guarantee that for both dyes the equilibrium would be attained even in higher biosorbate concentrations.

### 3.5. Equilibrium studies and mechanism of adsorption

An adsorption isotherm describes the relationship between the amount of adsorbate taken up by the adsorbent ($q_e$) and the

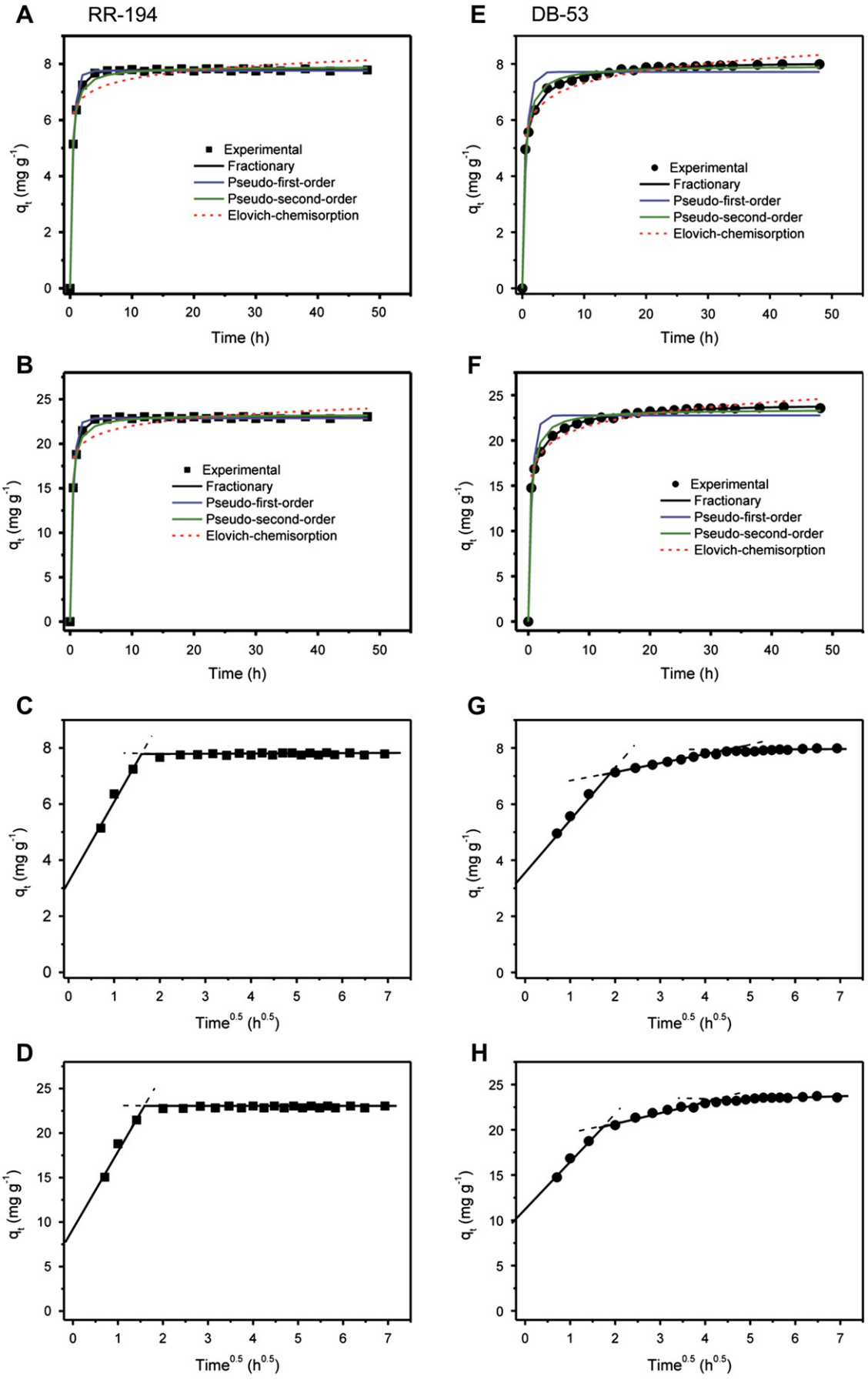


**Fig. 4.** Kinetic biosorption curves. A) RR-194, $C_o$ 20.0 mg $L^{-1}$; B) RR-194, $C_o$ 60.0 mg $L^{-1}$; C) RR-194, $C_o$ 20.0 mg $L^{-1}$; D) RR-194, $C_o$ 60.0 mg $L^{-1}$; E) DB-53, $C_o$ 20.0 mg $L^{-1}$; F) DB-53, $C_o$ 60.0 mg $L^{-1}$; G) DB-53, $C_o$ 20.0 mg $L^{-1}$; H) DB-53, $C_o$ 60.0 mg $L^{-1}$. Conditions: pH was fixed at 2.0; the biosorbent dosage was fixed at 2.5 g $L^{-1}$; and the temperature was fixed at 298 K.

**Table 3**
Kinetic parameters for RR-194 and DB-53 removal using CS as biosorbent. Conditions: temperature was fixed at 298 K; pH 2.0 biosorbent dosage of 2.5 g $L^{-1}$.

| | RR-194 | | DB-53 | |
|---|---|---|---|---|
| | 20.0 mg $L^{-1}$ | 60.0 mg $L^{-1}$ | 20.0 mg $L^{-1}$ | 60.0 mg $L^{-1}$ |
| Fractionary-order | | | | |
| $k_{AV}$ ($h^{-1}$) | 2.25 | 2.20 | 1.71 | 1.73 |
| $q_e$ (mg $g^{-1}$) | 7.79 | 22.9 | 8.04 | 24.1 |
| $n_{AV}$ | 0.652 | 0.685 | 0.367 | 0.334 |
| $R^2_{adj}$ | 0.9996 | 0.9995 | 0.9991 | 0.9997 |
| $F_{error}$ | 0.0312 | 0.0977 | 0.0513 | 0.0866 |
| Pseudo-first order | | | | |
| $k_f$ ($h^{-1}$) | 1.96 | 1.95 | 1.52 | 1.58 |
| $q_e$ (mg $g^{-1}$) | 7.76 | 22.9 | 7.71 | 22.8 |
| $R^2_{adj}$ | 0.9940 | 0.9951 | 0.9502 | 0.9438 |
| $F_{error}$ | 0.129 | 0.343 | 0.384 | 1.202 |
| Pseudo-second order | | | | |
| $k_s$ (g $mg^{-1}$ $h^{-1}$) | 0.518 | 0.176 | 0.331 | 0.115 |
| $q_e$ (mg $g^{-1}$) | 7.91 | 23.3 | 7.95 | 23.5 |
| $h_o$ (mg $g^{-1}$ $h^{-1}$) | 32.4 | 95.4 | 20.9 | 63.1 |
| $R^2_{adj}$ | 0.9965 | 0.9954 | 0.9914 | 0.9886 |
| $F_{error}$ | 0.0992 | 0.332 | 0.160 | 0.541 |
| Chemisorption | | | | |
| $\alpha$ (mg $g^{-1}$ $h^{-1}$) | $2.16 \times 10^6$ | $7.03 \times 10^6$ | $6.06 \times 10^3$ | $1.78 \times 10^4$ |
| $\beta$ (g $mg^{-1}$) | 2.38 | 0.811 | 1.57 | 0.530 |
| $R^2_{adj}$ | 0.9538 | 0.9509 | 0.9840 | 0.9889 |
| $F_{error}$ | 0.358 | 1.09 | 0.217 | 0.535 |
| Intra-particle diffusion | | | | |
| $k_{id}$ (mg $g^{-1}$ $h^{-0.5}$) | 2.92[a] | 8.90[a] | 0.271[b] | 0.962[b] |

[a] First stage.
[b] Second stage.

adsorbate concentration remaining in the solution after the system attained the equilibrium ($C_e$). There are several equations to analyze experimental adsorption equilibrium data. The equation parameters of these equilibrium models often provide some insight into the adsorption mechanism, the surface properties and affinity of the adsorbent. In this work, the Langmuir, the Freundlich, the Sips and the Radke–Prausnitz isotherm models were tested.

The isotherms of adsorption of RR-194 and DB-53 were carried out at 298 K on the CS biosorbent, using the best experimental conditions described previously (Table 4 and Fig. 5). Based on the $F_{error}$, the Sips model is the best isotherm model for both dyes. The Sips model showed in Table 4 presents the lowest $F_{error}$ values, which means that the $q$ fit by this isotherm model was close to the $q$ measured experimentally when compared with other isotherm models. For RR-194 the Langmuir and the Freundlich isotherm models were not suitably fitted, presenting $F_{error}$ values ranging from 3.37 to 26.0-fold higher than the $F_{error}$ values obtained by the Sips isotherm model. For DB-53, the Langmuir, the Freundlich and the Radke-Praunsnitz presented $F_{error}$ values ranging from 12.1 to 41.1-fold higher than the $F_{error}$ values obtained by the Sips isotherm model. Therefore, all these models mentioned above for RR-194 and DB-53 dyes, using CS as biosorbent, have no physical value. Only for RR-194, the Radke–Prausnitz presented a $F_{error}$ value 1.58-fold higher than the $F_{error}$ value obtained by the Sips isotherm model. Taking into account that the Sips isotherm model presented the lowest $F_{error}$ value for both dyes, this isotherm model was chosen as the best for describing the equilibrium of adsorption of RR-194 and DB-53

**Table 4**
Isotherm parameters for RR-194 and DB-53 biosorption, using CS as biosorbent. Conditions: temperature was fixed at 298 K; contact time was fixed at 10 and 20 h for RR-194 and DB-53, respectively; pH was fixed at 2.0; biosorbent dosage was fixed at 2.5 g $L^{-1}$.

| | RR-194 | DB-53 |
|---|---|---|
| Langmuir | | |
| $Q_{max}$ (mg $g^{-1}$) | 66.0 | 38.8 |
| $K_L$ (L $mg^{-1}$) | 0.203 | 1.66 |
| $R^2_{adj}$ | 0.9978 | 0.9475 |
| $F_{error}$ | 0.735 | 1.99 |
| Freudlich | | |
| $K_F$ ($mg \cdot g^{-1} \cdot (mg \cdot L^{-1})^{-1/n_F}$) | 23.1 | 24.8 |
| $n_F$ | 4.15 | 8.54 |
| $R^2_{adj}$ | 0.8669 | 06480 |
| $F_{error}$ | 5.67 | 5.15 |
| Sips | | |
| $Q_{max}$ (mg $g^{-1}$) | 64.1 | 37.5 |
| $K_S$ (L $mg^{-1}$) | 0.214 | 1.56 |
| $n_S$ | 0.890 | 0.549 |
| $R^2_{adj}$ | 0.9998 | 0.9998 |
| $F_{error}$ | 0.218 | 0.125 |
| Radke–Prausnitz | | |
| $Q_{max}$ (mg $g^{-1}$) | 75.4 | 48.5 |
| $K_{RP}$ (L $g^{-1}$) | 0.165 | 1.10 |
| $n_{RP}$ | 0.952 | 0.943 |
| $R^2_{adj}$ | 0.9995 | 0.9696 |
| $F_{error}$ | 0.345 | 1.51 |

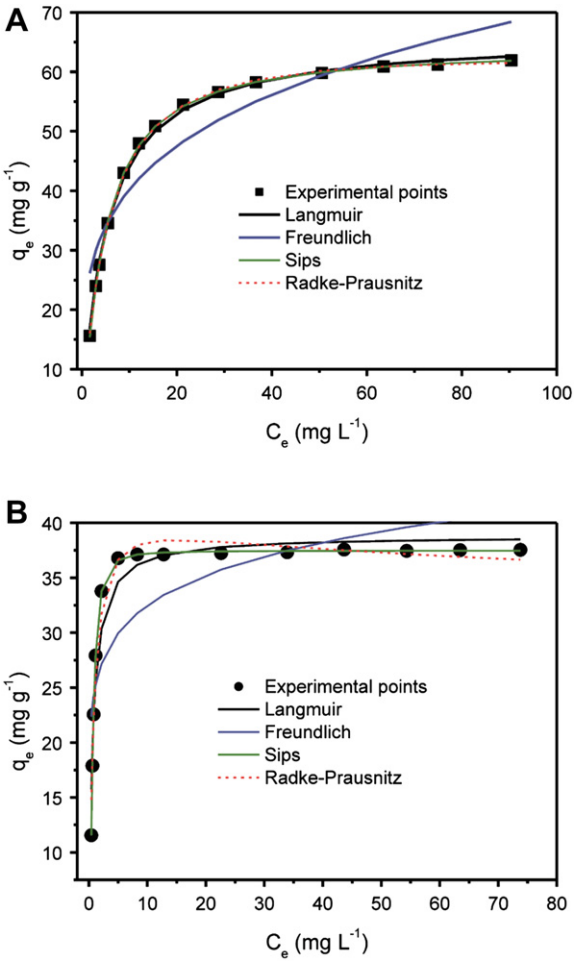


**Fig. 5.** Isotherm curves. A) RR-194; B) DB-53. Conditions: pH was fixed at 2.0; the biosorbent dosage was fixed at 2.5 g $L^{-1}$; and the temperature was fixed at 298 K. The contact time were fixed at 10 and 20 h for RR-194 and DB-53, respectively.

using CS as biosorbent. Therefore, based on the Sips isotherm model, the maximum amounts of RR-194 and DB-53 uptaken were 64.1 and 37.5 mg $g^{-1}$ for both dyes, respectively. These values indicate that CS is a fair good biosorbent for the removal of these dyes from aqueous solutions.

It should be highlighted that the maximum amount adsorbed of RR-194 by CS biosorbent was 70.9% higher than the value obtained for the adsorption of DB-53. Considering that the kinetics of adsorption of RR-194 was faster than the kinetics of adsorption of DB-53 as well as considering the pH studies showed above, it is possible to propose a mechanism of adsorption for RR-194 and DB-53, which is depicted in Fig. 6. In the first step, the CS is immersed in a solution with pH 2.0, being the functional groups (OH, carboxylates, please see Fig. 1) of the biosorbent protonated (see Fig. 3A and B). This step is fast for both dyes. The second step is the separation of the agglomerates of dyes in the aqueous solution. Dyes are in an organized state in the aqueous solution, besides being hydrated (Murakami, 2002). These self-associations of dyes in aqueous solutions should be dissociated before these dyes being adsorbed. Furthermore, the dyes should be dehydrated before being adsorbed. For RR-194 dye, this step is relatively fast. On the other hand, this stage is relatively slower for DB-53 (Murakami, 2002). This explains the differences of the minimum contact time for RR-194 and DB-53 to attain the equilibrium (see section 3.4). The third stage is the electrostatic attraction of the negatively charged dyes by the positively surface charged CS biosorbent at pH 2 (see Fig. 1). This stage should be the rate controlling step for RR-194. For DB-53, this is also the rate controlling step, however, the stage 2 presents some significance to overall mechanism of adsorption.

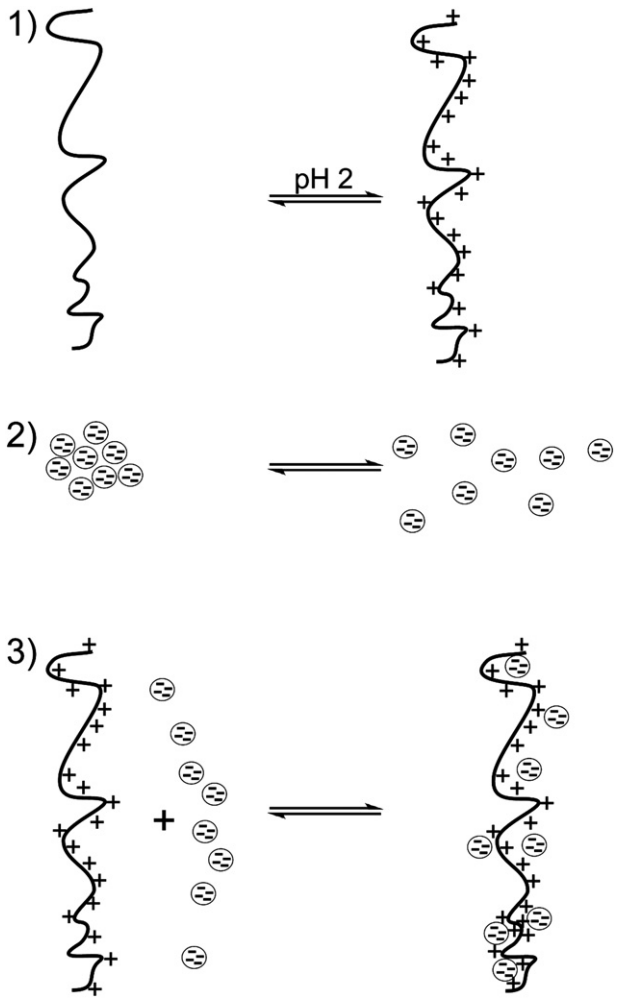


**Fig. 6.** Mechanism of biosorption of RR-194 and DB-53 dyes by the CS biosorbent. The circle stands for the dyes with four negative charges.

## 4. Conclusion

The cupuassu shell (CS; *T. grandiflorum*) is a good alternative biosorbent to remove C.I. Reactive Red 194 (RR-194) and C.I. Direct Blue 53 (DB-53) textile dyes from aqueous solutions. The CS was characterized by FTIR spectroscopy, SEM and nitrogen adsorption/desorption curves. It was demonstrated that the OH groups of phenols and alcohols and the carboxylate groups presented shift to lower wavenumber after contact with both dyes, indicating that these groups should participate of the biosorption mechanism.Both dyes interact with the biosorbent at the solid/liquid interface when suspended in water. The best conditions were established with respect to pH and contact time to saturate the available sites located on the adsorbent surface. Five kinetic models were used to adjust the adsorption and the best fit was the Avrami (fractionary-order) kinetic model. However, the intra-particle diffusion model gave multiple linear regions, which suggested that the biosorption may also be followed by multiple adsorption rates. The equilibration time for RR-194 and DB-53 dye were obtained after 8 and 18 h, respectively of contact between the dyes and the biosorbent. The equilibrium isotherm of these dyes was obtained, being these data better fitted to the Sips isotherm model. The maximum adsorption capacities were 64.1 and 37.5 mg $g^{-1}$ for RR-194 and DB-53, respectively, using CS biosorbent.

## Acknowledgements

The authors are grateful to Conselho Nacional de Desenvolvimento Científico e Tecnológico (CNPq), to Coordenação de Aperfeiçoamento de Pessoal de Nível Superior (CAPES), and to Fundação de Amparo à Pesquisa do Estado do Rio Grande do Sul (FAPERGS) for financial supports and fellowships. We are also grateful to Centro de Microscopia Eletrônica (CME-UFRGS) for the use of the SEM microscope.

## Nomenclature

| | |
|---|---|
| C | constant related with the thickness of boundary layer (mg $g^{-1}$). |
| $C_e$ | dye concentration at the equilibrium (mg $L^{-1}$). |
| $C_f$ | dye concentration at ending of the adsorption (mg $L^{-1}$). |
| $C_o$ | initial dye concentration put in contact with the adsorbent (mg $L^{-1}$). |
| $h_o$ | the initial sorption rate (mg $g^{-1}$ $h^{-1}$) of pseudo-second order equation. |
| $k_{AV}$ | is the Avrami kinetic constant $[(h^{-1})^{-n_{AV}}]$ |
| $K_F$ | the Freundlich equilibrium constant $[mg \cdot g^{-1} \cdot (mg \cdot L^{-1})^{-1/n_F}]$ |
| $k_f$ | the pseudo-first order rate constant ($h^{-1}$). |
| $k_{id}$ | the intra-particle diffusion rate constant (mg $g^{-1}$ $h^{-0.5}$). |
| $K_L$ | the Langmuir equilibrium constant (L $mg^{-1}$). |
| $K_{RP}$ | the Radke–Prausnitz equilibrium constant (L $mg^{-1}$) |
| $K_S$ | the Sips equilibrium constant (L $mg^{-1}$) |
| $k_s$ | the pseudo-second order rate constant (g $mg^{-1}$ $h^{-1}$). |
| $n_{AV}$ | is a fractionary reaction order (Avrami) which can be related, to the adsorption mechanism |
| $n_F$ | dimensionless exponent of the Freundlich equation |

$n_{RP}$ dimensionless exponent of the Radke–Prausnitz equation
$n_S$ dimensionless exponent of the Sips equation
$q$ amount adsorbed of the dye by the adsorbent (mg $g^{-1}$).
$q_e$ amount adsorbate adsorbed at the equilibrium (mg $g^{-1}$).
$Q_{max}$ the maximum adsorption capacity of the adsorbent (mg $g^{-1}$).
$q_t$ amount of adsorbate adsorbed at time (mg $g^{-1}$).
$t$ time of contact ($h$).
X biosorbent dosage (g $L^{-1}$).

*Greek letters*

$\alpha$ the initial adsorption rate (mg $g^{-1}$ $h^{-1}$) of the Elovich Equation
$\beta$ Elovich constant related to the extent of surface coverage and also to the activation energy involved in chemisorption (g $mg^{-1}$).

## Appendix. Supplementary material

Supplementary data related to this article can be found online at doi:10.1016/j.jenvman.2010.12.010.

## References


Akar, T., Ozcan, A.S., Tunali, S., Ozcan, A., 2008. Biosorption of a textile dye (Acid Blue 40) by cone biomass of Thuja orientalis: Estimation of equilibrium, thermodynamic and kinetic parameters. Bioresour. Technol. 99, 3057–3065.

Al-Degs, Y.S., El-Barghouthi, M.I., El-Sheikh, A.H., Walker, G.M., 2008. Effect of solution pH, ionic strength, and temperature on adsorption behavior of reactive dyes on activated carbon. Dyes Pigm. 77, 16–23.

Arenas, L.T., Lima, E.C., dos Santos Jr., A.A., Vaghetti, J.C.P., Costa, T.M.H., Benvenutti, E.V., 2007. Use of statistical design of experiments to evaluate the sorption capacity of 1,4-diazoniabicycle[2.2.2]octane/silica chloride for Cr(VI) adsorption. Colloids Surf. A 297, 240–248.

Baek, M.H., Ijagbemi, C.O., Se-Jin, O., Kim, D.S., 2010. Removal of Malachite green from aqueous solution using degreased coffee bean. J. Hazard. Mater. 176, 820–828.

Bekçi, Z., Seki, Y., Cavas, L., 2009. Removal of malachite green by using an invasive marine alga *Caulerpa racemosa* var. *cylindracea*. J. Hazard. Mater. 161, 1454–1460.

Blanachard, G., Maunaye, M., Martin, G., 1984. Removal of heavy metals from waters by means of natural zeolites. Water Res. 18, 1501–1507.

Brookstein, D.S., 2009. Factors associated with textile pattern dermatitis caused by contact allergy to dyes, finishes, foams, and preservatives. Dermatol. Clin. 27, 309–322.

Calvete, T., Lima, E.C., Cardoso, N.F., Dias, S.L.P., Pavan, F.A., 2009. Application of carbon adsorbents prepared from the Brazilian-pine fruit shell for removal of Procion Red MX 3B from aqueous solution - Kinetic, equilibrium, and thermodynamic studies. Chem. Eng. J. 155, 627–636.

Calvete, T., Lima, E.C., Cardoso, N.F., Vaghetti, J.C.P., Dias, S.L.P., Pavan, F.A., 2010. Application of carbon adsorbents prepared from Brazilian-pine fruit shell for the removal of reactive orange 16 from aqueous solution: kinetic, equilibrium, and thermodynamic studies. J. Environ. Manage. 91, 1695–1706.

Cestari, A.R., Vieira, E.F.S., Pinto, A.A., Lopes, E.C.N., 2005. Multistep adsorption of anionic dyes on silica/chitosan hybrid 1. Comparative kinetic data from liquid- and solid-phase models. J. Colloid Interface Sci. 292, 363–372.

Cestari, A.R., Vieira, E.F.S., Vieira, G.S., da Costa, L.P., Tavares, A.M.G., Loh, W., Airoldi, C., 2009. The removal of reactive dyes from aqueous solutions using chemically modified mesoporous silica in the presence of anionic surfactant-The temperature dependence and a thermodynamic multivariate analysis. J. Hazard. Mater. 161, 307–316.

Crini, G., 2006. Non-conventional low-cost adsorbents for dye removal: a review. Bioresou. Technol. 97, 1061–1085.

de Lima, R.O.A., Bazo, A.P., Salvadori, D.M.F., Rech, C.M., Oliveira, D.P., Umbuzeiro, G.A., 2007. Mutagenic and carcinogenic potential of a textile azo dye processing plant effluent that impacts a drinking water source. Mutat. Res. Genet. Toxicol. Environ. Mutagen 626, 53–60.

Deniz, F., Saygideger, S.D., 2010. Equilibrium, kinetic and thermodynamic studies of Acid Orange 52 dye biosorption by Paulownia tomentosa Steud. Leaf powder as a low-cost natural biosorbent. Bioresou. Technol. 101, 5137–5143.

Freundlich, H.M.F., 1906. Über die adsorption in lösungen. Z. Phys. Chem. 57A, 385–470.

Gay, D.S.F., Fernandes, T.H.M., Amavisca, C.V., Cardoso, N.F., Benvenutti, E.V., Costa, T.M.H., Lima, E.C., 2010. Silica grafted with a silsesquioxane containing the positively charged 1,4-diazoniabicyclo[2.2.2]octane group used as adsorbent for anionic dye removal. Desalination 258, 128–135.

Gondim, T.M.S., Thamazini, M.J., Calvacante, M.J.B., de Souza, J.M.L., 2001. Aspectos da produção de cupuaçu. Embrapa, Rio Branco-AC.

Gunay, A., 2007. Application of nonlinear regression analysis for ammonium exchange by natural (Bigadiç) clinoptilolite. J. Hazard. Mater. 148, 708–713.

Gupta, V.K., Suhas, I.A., 2009. Application of low-cost adsorbents for dye removal – A review. J. Environ. Manage. 90, 2313–2342.

Jacques, R.A., Bernardi, R., Caovila, M., Lima, E.C., Pavan, F.A., Vaghetti, J.C.P., Airoldi, C., 2007. Removal of Cu(II), Fe(III) and Cr(III) from aqueous solution by aniline grafted silica gel. Sep. Sci. Technol. 42, 591–609.

Janoš, P., Coskun, S., Pilařová, V., Rejnek, J., 2009. Removal of basic (Methylene Blue) and acid (Egacid Orange) dyes from waters by sorption on chemically treated wood shavings. Bioresour. Technol. 100, 1450–1453.

Kara, S., Aydiner, C., Demirbas, E., Kobya, M., Dizge, N., 2007. Modeling the effects of adsorbent dose and particle size on the adsorption of reactive textile dyes by fly ash. Desalination 212, 282–293.

Kumari, P., Sharma, P., Srivastava, S., Srivastava, M.M., 2006. Biosorption studies on shelled Moringa oleifera Lamarck seed powder: removal and recovery of arsenic from aqueous system. Int. J. Miner. Process 78, 131–139.

Langmuir, I., 1918. The adsorption of gases on plane surfaces of glass, mica and platinum. J. Am. Chem. Soc. 40, 1361–1403.

Largegren, S., 1898. About the theory of so-called adsorption of soluble substances. Kungliga Suensk Vetenskapsakademiens Handlingar 241, 1–39.

Lima, E.C., Fenga, P.G., Romero, J.R., de Giovani, W.F., 1998. Electrochemical behaviour of $[Ru(4,4'\text{-}Me_2bpy)_2(PPh_3)(H_2O)](ClO_4)_2$ in homogeneous solution and incorporated into carbon paste electrodes. Application to oxidation of benzylic compounds. Polyhedron 17, 313–318.

Lima, E.C., Barbosa- Jr., F., Krug, F.J., Tavares, A., 2002. Copper determination in biological materials by ETAAS using W-Rh permanent modifier. Talanta 57, 177–186.

Lima, E.C., Brasil, J.L., Santos, A.H.D.P., 2003. Evaluation of Rh, Ir, Ru, W-Rh, W-Ir, and W-Ru as permanent modifiers for the determination of lead in ashes, coals, sediments, sludges, soils, and freshwaters by electrothermal atomic absorption spectrometry. Anal. Chim. Acta 484, 233–242.

Lima, E.C., Royer, B., Vaghetti, J.C.P., Brasil, J.L., Simon, N.M., dos Santos Jr., A.A., Pavan, F.A., Dias, S.L.P., Benvenutti, E.V., da Silva, E.A., 2007. Adsorption of Cu(II) on Araucaria angustifolia wastes: determination of the optimal conditions by statistic design of experiments. J. Hazard. Mater. 140, 211–220.

Lima, E.C., Royer, B., Vaghetti, J.C.P., Simon, N.M., da Cunha, B.M., Pavan, F.A., Benvenutti, E.V., Veses, R.C., Airoldi, C., 2008. Application of Brazilian-pine fruit coat as a biosorbent to removal of reactive red 194 textile dye from aqueous solution, kinetics and equilibrium study. J. Hazard. Mater. 155, 536–550.

Lopes, E.C.N., dos Anjos, F.S.C., Vieira, E.F.S., Cestari, A.R., 2003. An alternative Avrami equation to evaluate kinetic parameters of the interaction of Hg(II) with thin chitosan membranes. J. Colloid Interface Sci. 263, 542–547.

Mittal, A., Mittal, J., Malviya, A., Kaur, D., Gupta, V.K., 2010. Adsorption of hazardous dye crystal violet from wastewater by waste materials. J. Colloid Interface Sci. 343, 463–473.

Murakami, K., 2002. Thermodynamic and kinetic aspects of self-association of dyes in aqueous solution. Dyes Pigm. 53, 31–43.

Olivares-Marín, M., Del-Prete, V., Garcia-Moruno, E., Fernández-González, C., Macías-García, A., Gómez-Serrano, V., 2009. The development of an activated carbon from cherry stones and its use in the removal of ochratoxin A from red wine. Food Control 20, 298–303.

Órfão, J.J.M., Silva, A.I.M., Pereira, J.C.V., Barata, S.A., Fonseca, I.M., Faria, P.C.C., Pereira, M.F.R., 2006. Adsorption of a reactive dye on chemically modified activated carbons-Influence of pH. J. Colloid Interface Sci. 296, 480–489.

Pavan, F.A., Gushikem, Y., Mazzocato, A.S., Dias, S.L.P., Lima, E.C., 2007. Statistical design of experiments as a tool for optimizing the batch conditions to methylene blue biosorption on yellow passion fruit and mandarin peels. Dyes Pigm. 72, 256–266.

Pavan, F.A., Dias, S.L.P., Lima, E.C., Benvenutti, E.V., 2008. Removal of congo red from aqueous solution by anilinepropylsilica xerogel. Dyes Pigm. 76, 64–69.

Radke, C.J., Prausnitz, J.M., 1972. Adsorption of organic solutes from dilute aqueous solution on activated carbon. Ind. Eng. Chem. Fundam. 11, 445–451.

Rosa, S., Laranjeira, M.C.M., Riela, H.G., Fávere, V.T., 2008. Cross-linked quaternary chitosan as an adsorbent for the removal of the reactive dye from aqueous solutions. J. Hazard. Mater. 155, 253–260.

Rosenkranz, H.S., Cunningham, S.L., Mermelstein, R., Cunningham, A.R., 2007. The challenge of testing chemicals for potential carcinogenicity using multiple short-term assays: an analysis of a proposed test battery for hair dyes. Mutat. Res. Genet. Toxicol. Environ. Mutagen 633, 55–66.

Royer, B., Cardoso, N.F., Lima, E.C., Ruiz, V.S.O., Macedo, T.R., Airoldi, C., 2009a. Organofunctionalized kenyaite for dye removal from aqueous solution. J. Colloid Interface Sci. 336, 398–405.

Royer, B., Cardoso, N.F., Lima, E.C., Vaghetti, J.C.P., Simon, N.M., Calvete, T., Veses, R.C., 2009b. Applications of Brazilian-pine fruit shell in natural and carbonized forms as adsorbents to removal of methylene blue from aqueous solutions - Kinetic and equilibrium study. J. Hazard. Mater. 164, 1213–1222.

Royer, B., Cardoso, N.F., Lima, E.C., Macedo, T.R., Airoldi, C., 2010a. A useful organofunctionalized layered silicate for textile dye removal. J. Hazard. Mater. 181, 366–374.

Royer, B., Cardoso, N.F., Lima, E.C., Macedo, T.R., Airoldi, C., 2010b. Sodic and acidic crystalline lamellar magadiite adsorbents for removal of methylene blue from aqueous solutions. Kinetic and equilibrium studies. Sep. Sci. Technol. 45, 129–141.

Royer, B., Lima, E.C., Cardoso, N.F., Calvete, T., Bruns, R.E., 2010c. Statistical design of experiments for optimization of batch adsorption conditions for removal of reactive red 194 textile dye from aqueous effluents. Chem. Eng. Commun. 197, 775–790.

Sips, R., 1948. On the structure of a catalyst surface. J. Chem. Phys. 16, 490–495.

Smith, B., 1999. Infrared Spectral Interpretation – A Systematic Approach. CRC Press, Boca Raton.

Vaghetti, J.C.P., Lima, E.C., Royer, B., Brasil, J.L., da Cunha, B.M., Simon, N.M., Cardoso, N.F., Noreña, C.P.Z., 2008. Application of Brazilian-pine fruit coat as a biosorbent to removal of Cr(VI) from aqueous solution. Kinetics and equilibrium study. Biochem. Eng. J. 42, 67–76.

Vaghetti, J.C.P., Lima, E.C., Royer, B., da Cunha, B.M., Cardoso, N.F., Brasil, J.L., Dias, S.L.P., 2009. Pecan nutshell as biosorbent to remove Cu(II), Mn(II) and Pb (II) from aqueous solutions. J. Hazard. Mater. 162, 270–280.

Vieira, A.P., Santana, S.A.A., Bezerra, C.W.B., Silva, H.A.S., Chaves, J.A.P., de Melo, J.C.P., Silva-Filho, E.C., Airoldi, C., 2009. Kinetics and thermodynamics of textile dye adsorption from aqueous solutions using babassu coconut mesocarp. J. Hazard. Mater. 166, 1272–1278.

Weber Jr., W.J., Morris, J.C., 1963. Kinetics of adsorption on carbon from solution. J. Sanit. Eng. Div. Am. Soc. Civil Eng. 89, 31–59.

Yurtsever, M., Sengil, I.A., 2009. Biosorption of Pb(II) ions by modified quebracho tannin resin. J. Hazard. Mater. 163, 58–64.